The hydrogen atom in a semi-infinite space limited by a paraboloidal boundary

1991 J. Phys. A: Math. Gen. 24 1481

(http://iopscience.iop.org/0305-4470/24/7/021)

J. Phys. A: Math. Gen. **24** (1991) 1481–1493. Printed in the UK

The hydrogen atom in a semi-infinite space limited by a paraboloidal boundary

E Ley-Koo and R M G García-Castelán

Instituto de Física, Universidad Nacional Autónoma de México, Apartado Postal 20-364, 01000 México, DF, México

Received 6 April 1990, in final form 12 June 1990

Abstract. The hydrogen atom in a semi-infinite space limited by a paraboloidal boundary, with the nucleus at the focus, is studied as a model of an atom on the surface of a solid. The energy eigenvalues, hyperfine structure, electric dipole moment and pressure of the system are evaluated as the paraboloidal boundary approaches the nucleus up to the position at which the atom becomes ionized.

1. Introduction

In this paper we formulate and solve exactly the problem of the hydrogen atom in a semi-infinite space limited by a paraboloidal surface. This system is of interest as a model of an atom on the surface of a solid. We have become involved with such models in connection with the study of electron emission by compressed rocks (Shevtsov *et al* 1975, Brady and Rowell 1986, Guo *et al* 1988, Ley-Koo *et al* 1989). More generally, the development of these models is important for the study of surface physical phenomena (Levine 1965, Jiang and Shan 1985, Shan *et al* 1985, 1987, Shan 1987, 1990, Liu and Lin 1983, Satpathy 1983).

There is evidence for the emission of electrons in rocks under compression up to the point of fracture. Shevtsov *et al* (1975) detected and collected positive electric charges from the surface of feldspar samples under pressures from 0 to 80 MPa. Brady and Rowell (1986) observed the characteristic light of various atmospheres surrounding fracturing granite (at 300 MPa) and basalt samples, and concluded that the exoelectron excitation of the ambient atmosphere is responsible for such light emissions. Guo *et al* (1988) reported the direct detection of electrons with a Geiger–Müller counter in fracturing granite samples (at 170 MPa). Ley-Koo *et al* (1989) have proposed a possible mechanism, based on models of compressed atoms (Ley-Koo and Rubinstein 1979), for the production of electrons in rocks under compression. Models of atoms in boxes with penetrable walls (Ley-Koo and Rubinstein 1979) are capable of accounting for the production of electrons before and at the moment of fracture, with energies up to the order or one atomic unit, at pressures consistent with those of the experiments. The high-energy electrons reported by Guo *et al* (1988) cannot be directly explained through the mechanism of compressed atoms, since the pressures would have to be unrealistically high for the electrons to attain such energies. As pointed out by Ley-Koo *et al* (1989), additional experimental and theoretical work on the problem is needed. The energy distributions of the electrons before and at the moment of fracture need to be measured with the appropriate instrumentation. Models of atoms on the surface of the compressed solid sample must be developed and may serve as points of reference in the analysis of the problem under consideration.

The present investigation is the starting point of the line of inquiry stated at the end of the previous paragraph. An atom inside a solid has been modelled as an atom inside finite volumes (Michels *et al* 1937, Ley-Koo and Rubinstein 1979, 1980, Ley-Koo and Cruz 1981); the walls of the chosen volume simulate the confining effect on the atom due to its neighbouring atoms in the solid. An atom on the surface of a solid, on the other hand, can be modelled as an atom in a semi-infinite space, since its neighbouring atoms lay only inside the solid. Models of atoms in semi-infinite spaces have been investigated in solid state physics to study donor atoms on semiconductor surfaces (Levine 1965, Jiang and Shan 1985, Shan *et al* 1985, 1987, Shan 1990) and Wannier excitons near a semiconductor surface (Liu and Lin 1983, Satpathy 1983). A qualitative difference between these models and the ones we propose to study is that the semi-infinite space of interest is the inside of the solid in the former and the outside of the solid in the latter. Also in those models, the semi-infinite space is bounded by a plane, while in the problem of the rocks a curved surface is more appropriate.

Here we investigate the hydrogen atom in a semi-infinite space limited by a paraboloidal surface, with the nucleus at the focus. This model is related to the model of hydrogen atoms inside a box with paraboloidal surfaces (Ley-Koo and Rubinstein 1980) as the limit of the latter in which one of the surfaces is moved out to infinity. Qualitatively both problems are different, but their quantitative solutions are based on the same equations and methods. Consequently, in section 2 we borrow the equations of Ley-Koo and Rubinstein (1980) and solve them for the boundary conditions of the atom in the semi-infinite space to obtain the energy eigenvalues and eigenfunctions of the lowest states of the system. In section 3, we obtain the expressions to evaluate the hyperfine splitting, the electric dipole moment and the pressure of the atom in the ground state for different positions of the paraboloidal boundary. Numerical results for these properties are presented in section 4 together with a discussion of their changes as the paraboloidal surface approaches the nucleus up to the point at which the electron abandons the atom. In the appendix we give the detail to evaluate the integrals in the anisotropic hyperfine splitting.

2. Energy eigenvalues and eigenfunctions

In the notation of Ley-Koo and Rubinstein (1980) we use parabolic coordinates ($\xi = r - z$, $\eta = r + z$, φ) to define the position of the electron relative to the nucleus in the hydrogen atom. The eigenvalue problem for the hydrogen atom in a semi-infinite space limited by the paraboloidal surface, $\xi = \xi_0$, is defined by the Schrödinger equation

$$\left\{-\frac{\hbar^2}{2\mu}\left[\frac{4}{\xi+\eta}\left(\frac{\partial}{\partial\xi}\xi\frac{\partial}{\partial\xi}+\frac{\partial}{\partial\eta}\eta\frac{\partial}{\partial\eta}\right)+\frac{1}{\xi\eta}\frac{\partial^2}{\partial\varphi^2}\right]-\frac{2Ze^2}{\xi+\eta}\right\}\psi(\xi,\eta,\varphi)=E\psi(\xi,\eta,\varphi) \tag{1}$$

and the boundary conditions

$$\psi(\xi=\xi_0,\eta,\varphi)=0 \tag{2a}$$

$$\psi(\xi,\eta\to\infty,\varphi)=0 \tag{2b}$$

on the wavefunction.

Equation (1) is separable and admits the factorized solution (Buckingham 1961)

$$\psi(\xi,\eta,\varphi)=C\Xi(\xi)H(\eta)\Phi(\varphi). \tag{3}$$

The factor depending on the azimuthal angle corresponds to eigenstates of the axial component of the orbital angular momentum

$$\Phi(\varphi)=\frac{e^{im\varphi}}{\sqrt{2\pi}} \tag{4a}$$

$$m=0, \pm 1, \pm 2, \ldots \tag{4b}$$

i.e. σ, π, $\delta, \ldots$ states. The other factors satisfy the ordinary differential equations

$$\left[-\frac{\hbar^2}{2\mu}\left(\frac{4}{\xi}\frac{d}{d\xi}\xi\frac{d}{d\xi}-\frac{m^2}{\xi^2}\right)-\frac{4K_1}{\xi}\right]\Xi=E\Xi \tag{5a}$$

$$\left[-\frac{\hbar^2}{2\mu}\left(\frac{4}{\eta}\frac{d}{d\eta}\eta\frac{d}{d\eta}-\frac{m^2}{\eta^2}\right)-\frac{4K_2}{\eta}\right]H=EH \tag{5b}$$

where the separation constants K_1 and K_2 are constrained by the relation

$$K_1+K_2=\frac{Ze^2}{2}. \tag{6}$$

Both equations (5a) and (5b) are mathematically of the same type and can be dealt with at the same time by introducing the independent variable q_i and the function Q_i, with $i=1, 2$ corresponding to the situations of ξ and η, respectively. The regular singular point $q_i=0$ is removed by taking

$$Q_i(q_i)=q_i^{|m|/2}f(q_i) \tag{7}$$

after which equations (5) transform into

$$\left(\frac{d^2}{dq_i^2}+\frac{|m|+1}{q_i}\frac{d}{dq_i}+\frac{2\mu K_i}{\hbar^2 q_i}+\frac{2\mu E}{\hbar^2}\right)f(q_i)=0. \tag{8}$$

In terms of the Bohr radius, $a_0=\hbar^2/\mu e^2$, and the energy parameter ν, such that

$$E=-\frac{Z^2e^2}{2a_0\nu^2} \tag{9}$$

it is convenient to introduce the dimensionless variables

$$\rho_i=\frac{Zq_i}{2a_0\nu} \tag{10}$$

and to reparametrize the separation constants:

$$\frac{2\mu K_i}{\hbar^2}=\frac{Z}{a_0}\frac{\nu_i+\frac{1}{2}(|m|+1)}{\nu}. \tag{11}$$

Then equations (6) and (8) become

$$\nu_1+\nu_2+|m|+1=\nu \tag{12}$$

and

$$\left(\frac{d^2}{d\rho_i^2}+\frac{|m|+1}{\rho_i}\frac{d}{d\rho_i}+\frac{2\nu_i+|m|+1}{\rho_i}-1\right)f(\rho_i)=0. \tag{13}$$

The solutions of equation (13) are well known. For $i=1$, we use the power series expansion developed by Ley-Koo and Rubinstein (1980)

$$f(\rho_1)=\sum_{s=0}^{\infty} c_s^{(m)}\rho_1^s \tag{14}$$

with the recurrence relation following from equation (13),

$$\begin{aligned} c_{N+1}^{(m)} &= -\frac{(2\nu_1+|m|+1)c_N^{(m)}-c_{N-1}^{(m)}}{(N+1)(N+|m|+1)} \qquad N=1,2,3,\ldots \\ c_1^{(m)} &= -\frac{2\nu_1+|m|+1}{|m|+1} \qquad c_0^{(m)}=1. \end{aligned} \tag{15}$$

For $i=2$, we use the solution in terms of the confluent hypergeometric function

$$f(\rho_2)=\mathrm{e}^{-\rho_2}\,{}_1F_1(-\nu_2,|m|+1,2\rho_2). \tag{16}$$

The energy eigenvalues (equations (9) and (12)) and the eigenfunctions (equations (3), (4), (7), (14) and (16)) are determined by the boundary conditions (equations (2*a*) and (2*b*)), which take the explicit forms

$$\sum_{s=0}^{\infty} c_s^{(m)}\left(\frac{Z\xi_0}{2a_0\nu}\right)^s=0 \tag{17}$$

from (14), and

$$\nu_2=0,1,2,3,\ldots \tag{18}$$

from (16), respectively. For chosen values of the position of the paraboloidal boundary, ξ_0, and of the quantum numbers m and ν_2, equation (17) can be satisfied only for discrete values of ν_1, since the coefficients $c_s^{(m)}$ (equation (15)) and the energy parameter ν (equation (12)) depend explicitly on ν_1. This results in discrete values for the energy (equation (9)).

In order to carry out the numerical calculations for a given choice of m and ν_2 we start by fixing the value of ν_1. Then the values of ν (equation (12)) and of the energy equation (9) are also fixed. Thus the coefficients of equation (15) can be generated, and the zeros of the sum of equation (14) can be obtained to the desired accuracy with the necessary finite number of terms. The corresponding zeros ρ_{10} determine the positions of the paraboloidal boundaries

$$\xi_0=\frac{2a_0\nu\rho_{10}}{Z} \tag{19}$$

of the semi-infinite spaces for which the eigenvalue problem of the hydrogen atom has been solved.

It is of special interest to determine the position of the paraboloidal surface limiting the semi-infinite space for which the hydrogen atom becomes ionized. We go back to equation (5*a*) taking the vanishing value of the energy, $E=0$, corresponding to the limit $\nu\to\infty$, $\nu_1\to\infty$, for which, according to equations (11) and (6), $K_1=Ze^2/2$ and $K_2=0$. With the additional change of variable

$$x=2\sqrt{\frac{Z\xi}{a_0}} \tag{20}$$

equation (5*a*) becomes the ordinary Bessel equation (Abramowitz and Stegun 1965)

$$\left(x^2\frac{\mathrm{d}^2}{\mathrm{d}x^2}+x\frac{\mathrm{d}}{\mathrm{d}x}+(x^2-m^2)\right)\Xi=0. \tag{21}$$

Then the boundary condition equation (2a) gives the position of the paraboloidal boundary

$$\xi_0 = \frac{a_0 j_{m,n}^2}{4Z} \tag{22}$$

in terms of the zeros of the regular Bessel function of order m. The successive zeros, $n = 1, 2, 3, \ldots$, correspond to the successive orders of excitation of the degree of freedom associated with the ξ-coordinate. Notice that the limit situation analysed above is independent of the order of excitation of the degree of freedom associated with the η-coordinate (equation (18)). This means that all the eigenstates $\psi_{n\nu_2 m}$ with fixed values of n and m, but different values of ν_2 tend to become ionized for the same position (equation (22)) of the paraboloidal boundary of the semi-infinite space.

3. Ground state properties

In this section we evaluate the hyperfine splitting, the electric dipole moment and the pressure of the confined atomic hydrogen in its ground state,

$$\psi_{\nu,00}(\xi, \eta, \varphi) = \frac{C}{\sqrt{2\pi}} \mathrm{e}^{-\rho_2} \sum_{s=0}^{\infty} c_s^{(0)} \rho_1^s \tag{23}$$

as a function of the position ξ_0 of the confining wall.

The isotropic hyperfine splitting is given by the Fermi contact term (Atherton 1973)

$$A_{\mathrm{iso}} = \frac{8\pi}{3} g_e \beta g_N \beta_N |\psi(0)|^2 = \tfrac{4}{3} g_e \beta g_N \beta_N C^2 \tag{24}$$

and requires the evaluation of the normalization constant C in equation (23). This is accomplished by imposing the normalization condition on the wavefunction of equation (23),

$$\begin{aligned} 1 &= \int |\psi(\xi, \eta, \varphi)|^2 \, \mathrm{d}V \\ &= \frac{C^2}{4}\left(\frac{2a_0\nu}{z}\right)^3 \sum_{p=0}^{\infty}\left(\sum_{t=0}^{p} c_{p-t}^{(0)} c_t^{(0)}\right)\left(\frac{\rho_{10}^{p+2}}{2(p+2)} + \frac{\rho_{10}^{p+1}}{4(p+1)}\right). \end{aligned} \tag{25}$$

For a chosen value of ν_1, the energy parameter ν (equation (12)), the coefficients $c_s^{(0)}$ (equation (15)) and the zeros ρ_{10} of equation (14) are numerically determined as indicated in section 2. Thus the numerical evaluation of A_{iso} (equation (24)) can also be accomplished by carrying out the summations in equation (25).

The axial anisotropic component of the hyperfine splitting is given by the expectation value of the corresponding component of the dipole–dipole operator (Atherton 1973),

$$\begin{aligned} A_{33}^0 &= g_e \beta g_N \beta_N \left\langle \psi \left| \frac{3Z^2 - r^2}{r^5} \right| \psi \right\rangle \\ &= 4 g_e \beta g_N \beta_N C^2 \sum_{p=0}^{\infty} \left(\sum_{t=0}^{p} c_{p-t}^{(0)} c_t^{(0)} \right) \\ &\quad \times \int_0^{\rho_{10}} \int_0^{\infty} \rho_1^p \, \mathrm{e}^{-2\rho_2} \frac{\rho_1^2 - 4\rho_1\rho_2 + \rho_2^2}{(\rho_1 + \rho_2)^4} \, \mathrm{d}\rho_1 \, \mathrm{d}\rho_2. \end{aligned} \tag{26a}$$

The last double integral has an integrand with the integrable singularity at $\rho_1=0$, $\rho_2=0$, which according to the method of Stephen and Auffray (1959) gives the contribution

$$\lim_{k\to 0}\int_0^k \mathrm{d}\rho_1\,\rho_1^p\int_{k-\rho_1}^k \mathrm{d}\rho_2\,\mathrm{e}^{-2\rho_2}\frac{\rho_1^2-4\rho_1\rho_2+\rho_2^2}{(\rho_1+\rho_2)^4}=\tfrac{1}{6}\delta_{p,0}. \tag{27a}$$

The remaining integration

$$T_p(\rho_{10})=\lim_{k\to 0}\int_k^{\rho_{10}}\int_0^\infty \rho_1^p\,\mathrm{e}^{-2\rho_2}\frac{\rho_1^2-4\rho_1\rho_2+\rho_2^2}{(\rho_1+\rho_2)^2}\,\mathrm{d}\rho_1\,\mathrm{d}\rho_2 \tag{27b}$$

is evaluated in the appendix and reduced to a form (equation (A5)) which can be computed numerically. The contributions of equations (27a) and (27b) to the double integral in equation (26a) transform the latter into

$$A_{33}^0=\tfrac{1}{2}A_{\mathrm{iso}}+4g_e\beta g_N\beta_N C^2\sum_{p=0}^\infty\left(\sum_{t=0}^p c_{p-t}^{(0)}c_t^{(0)}\right)T_p(\rho_{10}) \tag{26b}$$

where it is recognized that the contribution from the integrable singularity is half the value of equation (24) and that all the factors and coefficients in the second term are also known.

The expectation value of the electric dipole moment of the confined hydrogen atom, $-e\langle \boldsymbol{r}\rangle$, has only a non-vanishing axial component due to the invariance of the system under rotations around the axis of the confining paraboloidal surface:

$$\boldsymbol{d}=-e\langle z\rangle\hat{k}=-\hat{k}e\frac{C^2}{8}\left(\frac{2a_0\nu}{Z}\right)^4\sum_{p=0}^\infty\left(\sum_{t=0}^p c_{p-t}^{(0)}c_t^{(0)}\right)\left(\frac{\rho_{10}^{p+1}}{4(p+1)}-\frac{\rho_{10}^{p+3}}{2(p+3)}\right). \tag{28}$$

Concerning the pressure in confined atoms, it must be recognized that since the original work of Michels *et al* (1937) such a pressure has been evaluated only for the case of s states in spherical boxes, for which the pressure is uniform due to the symmetry of both the state and the box. If one considers p states in spherical boxes, it is realized that the pressure is not uniform, vanishing in the nodal equator and increasing towards the poles, as determined by the angular variations of the electron probability density. Correspondingly, in the system under consideration in this paper, the pressure is not uniform in the different points of the paraboloidal surface bounding the semi-infinite space. In order to evaluate the pressure in each point, we introduce the energy density (Hirschfelder 1978)

$$\varepsilon(\xi_0,\eta,\varphi)\,\Delta\eta\,\Delta\varphi=\left(\int_0^{\xi_0}h_\xi h_\eta h_\varphi\,\mathrm{d}\xi\,\psi^*\hat{H}\psi\right)\Delta\eta\,\Delta\varphi \tag{29}$$

associated with a cylinder-like element around the points with a sectional area $h_\eta h_\varphi\,\Delta\eta\,\Delta\varphi$ from $\xi=0$ to $\xi=\xi_0$, where the h are the scale factors associated with the respective coordinates. The relative change in the energy equation (29) as the paraboloidal boundary is changed infinitesimally, divided by the area of the cross section of the element gives the pressure

$$\begin{aligned}P(\xi_0,\eta,\varphi)&=-\frac{1}{h_\eta h_\varphi\,\Delta\eta\,\Delta\varphi}\frac{1}{h_\xi}\frac{\partial}{\partial\xi_0}\varepsilon(\xi_0,\eta,\varphi)\,\Delta\eta\,\Delta\varphi\\&=-\frac{4}{\xi+\eta}\frac{\partial}{\partial\xi_0}\varepsilon(\xi_0,\eta,\varphi).\end{aligned} \tag{30}$$

By using the explicit form of the ground state wavefunction (equation (23)), and the fact that it is an eigenfunction of the Hamiltonian operator with the eigenvalues of equation (9), then the energy density function of equation (29) becomes

$$\varepsilon(\xi_0, \eta) = \frac{C^2}{2\pi} E(\xi_0) \int_0^{\xi_0} (\xi+\eta)\, d\xi [\Xi(\xi)]^2 e^{-2\rho_2}$$
$$= -\frac{C^2}{8\pi} \frac{Z^2 e^2}{2a_0\nu^2}\left(\frac{2a_0\nu}{Z}\right)^2 e^{-2\rho_2} \sum_{p=0}^{\infty}\left(\sum_{t=0}^{p} c_{p-t}^{(0)} c_t^{(0)}\right)\left(\frac{\rho_{10}^{p+2}}{p+2} + \rho_2 \frac{\rho_{10}^{p+1}}{p+1}\right). \quad (31)$$

By using equations (25) and (31) the pressure of equation (30) takes the form

$$P(\xi_0, \eta) = \frac{Z^5 e^2}{4\pi a_0^4 \nu^2} \frac{e^{-2\rho_2}}{\rho_{10}+\rho_2}$$
$$\times \frac{\partial}{\partial \rho_{10}}\left(\frac{\sum_{p=0}\left(\sum_{t=0}^{p} c_{p-t}^{(0)} c_t^{(0)}\right)\left(\frac{\rho_{10}^{p+2}}{p+2} + \rho_2 \frac{\rho_{10}^{p+1}}{p+1}\right)}{\nu^3 \sum_{p=0}^{\infty}\left(\sum_{t=0}^{p} c_{p-t}^{(0)} c_t^{(0)}\right)\left(\frac{\rho_{10}^{p+2}}{p+2} + \frac{\rho_{10}^{p+1}}{2(p+1)}\right)}\right). \quad (32)$$

The fraction inside the brackets as well as its derivative can be calculated numerically as a function of ρ_{10}, for chosen values of ρ_2.

4. Results and discussion

Some illustrative numerical results for the energy eigenvalues, hyperfine splitting, electric dipole moment and pressure of the hydrogen atom in semi-infinite spaces are presented in the following tables and figures, as functions of the position of the paraboloidal surface boundary.

Table 1 contains the numerical values of the energy (equation (9)), and the energy parameters (12) and (18), for the lowest states of the hydrogen atom and different

Table 1. Energy and energy parameters for the lowest states of the hydrogen atom in a semi-infinite space bounded by different paraboloidal surfaces.

$(n_1 n_2 m)$	$E\ (e^2/2a_0)$	ν	ν_1	ν_2	$\xi_0\ (a_0)$
(00σ)	−1.00000	1	0	0	∞
	−0.99980	1.0001	0.0001	0	11.5565
	−0.84168	1.09	0.09	0	3.8345
	−0.27701	1.9	0.9	0	2.0475
	−0.17361	2.4	1.4	0	1.8678
	−0.01384	8.5	7.5	0	1.5381
(01σ)	−0.25000	2	0	1	∞
	−0.24752	2.01	0.01	1	12.5540
	−0.18904	2.3	0.3	1	4.8310
	−0.09183	3.3	1.3	1	2.7182
	−0.01208	9.1	7.1	1	1.7335
	−0.00346	17	15	1	1.5862
(10σ)	−0.25000	1	0	0	∞
	−0.24876	2.005	1.005	0	24.6928
	−0.12755	2.8	1.8	0	10.6677
	−0.06250	4	3	0	9.1771
	−0.01876	7.3	6.3	0	8.2858
	−0.01384	8.5	7.5	0	8.1704

positions (equations (17) and (19)) of the paraboloidal boundary of the semi-infinite space. The states are designated with the notation $(n_1 n_2 m)$ in terms of the order of excitation of the respective degrees of freedom. In the limit in which the boundary is very far, the energy of the states approaches the value for the free hydrogen atom with principal quantum number $n = n_1 + n_2 + |m| + 1$. While table 1 is restricted to the lowest σ states, figure 1(a) contains the corresponding energy curves for these and other σ states, and figures 1(b) and 1(c) correspond to π and δ states, respectively. If these curves are followed starting from large values of ξ_0, i.e. when the paraboloidal boundary is very far, the energies are close to the free hydrogen atom energy values and have

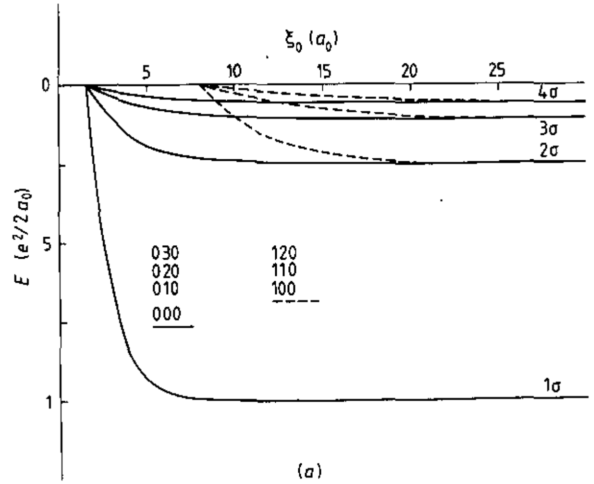

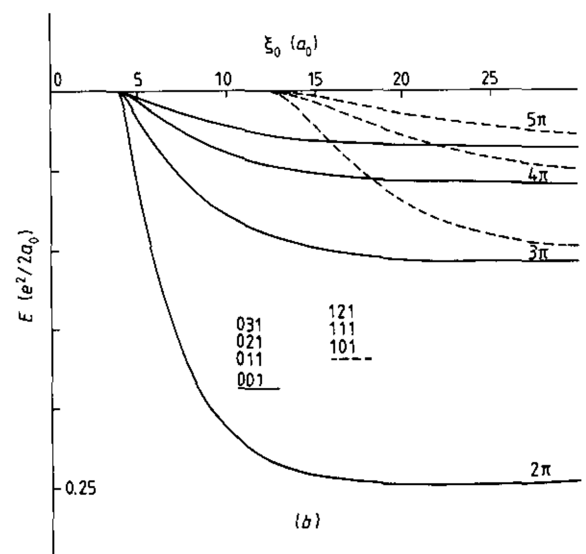

Figure 1. (a) Energy of lowest σ states of the hydrogen atom in a semi-infinite space bounded by different paraboloidal surfaces. (b) Energy of lowest π states of the hydrogen atom in a semi-infinite space bounded by different paraboloidal surfaces. (c) Energy of lowest δ states of the hydrogen atom in a semi-infinite space bounded by different paraboloidal surfaces.

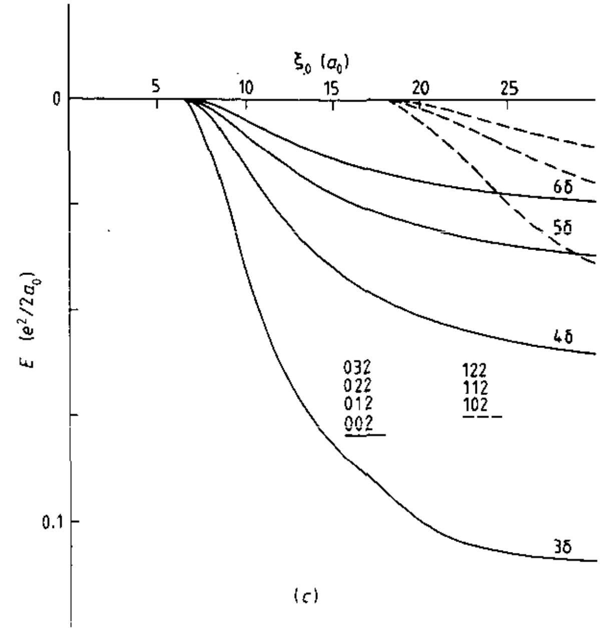

Figure 1. (continued)

the degeneracy n_1+n_2+1. As the paraboloidal boundary gets closer, ξ_0 taking smaller values, the degeneracy is removed and the energies increase monotonically due to the confinement effect. When the paraboloidal boundary takes the positions given by equation (22), the corresponding states have zero energy, becoming degenerate, and the atom is at the threshold of ionization.

Table 2 gives the numerical values of the isotropic and anisotropic components of the hyperfine splitting, the electric dipole moment and the pressure of the hydrogen atom in the ground state for different positions of the paraboloidal surface boundary. Figure 2(a) gives the variation of the isotropic hyperfine splitting equations (24) and (25)) as a function of ξ_0. It starts from the value of 50.762 mT for the free hydrogen atom for large values of ξ_0, increases slowly at first and then more rapidly as the paraboloidal surface is placed closer in; eventually, A_{iso} reaches a maximum and then

Table 2. Isotropic and anisotropic components of hyperfine splitting, electric dipole moment and pressure for the hydrogen atom in a semi-infinite space.

ξ_0 (a_0)	$A_{\mathrm{iso}}/g_e\beta$ (mT)	$A^0_{33}/g_e\beta$ (mT)	d ($-ea_0$)	P ($\rho_2=0$) (10^{13} Pa)	P ($\rho_2=1$) (10^{13} Pa)
10.0100	50.8918	0.0000	0.0041	1.6200	0.2700
6.4312	53.4566	0.0000	0.1026	0.0514	0.0045
3.8345	61.8536	0.0402	0.3976	0.0164	0.0035
1.8678	30.3252	2.7534	2.0051	0.0051	0.0020
1.7871	23.8069	2.4572	2.4199	0.0032	0.0011
1.6631	13.0265	2.1811	3.6430	0.0009	0.0005
1.5548	4.3488	1.1144	6.9636	0.00012	0.00009
1.5381	3.2633	0.8999	8.16685	0.00011	0.00005

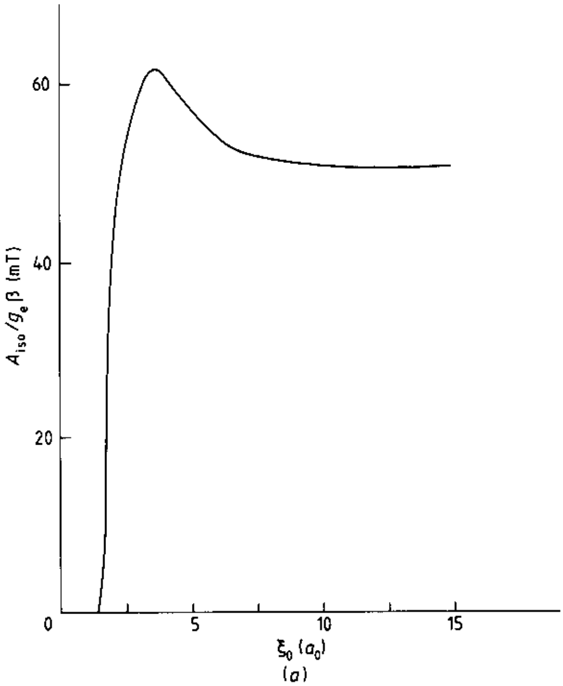

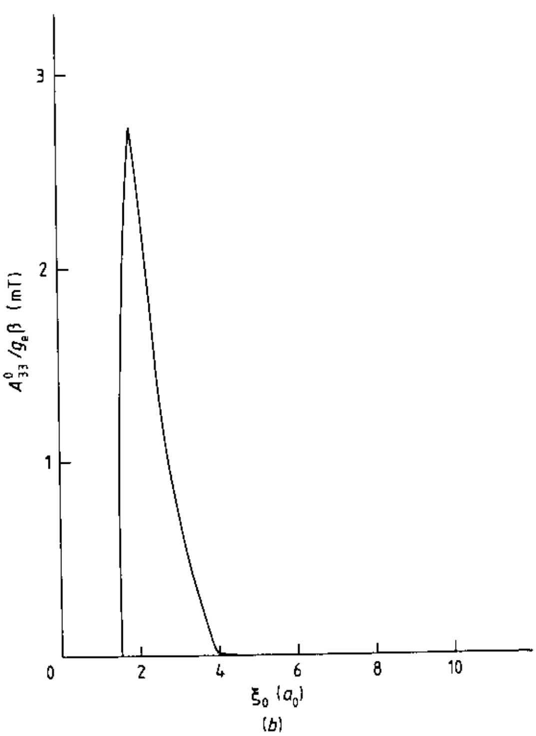

Figure 2. (*a*) Isotropic hyperfine splitting of the hydrogen atom in a semi-infinite space bounded by different paraboloidal surfaces. (*b*) Anisotropic hyperfine splitting of the hydrogen atom in a semi-infinite space bounded by different paraboloidal surfaces.

drops to zero fairly rapidly as the boundary approaches the position at which the atom becomes ionized. The increase in the values of A_{iso} reflects the increase of the probability of finding the electron at the position of the nucleus due to the confiment effect of the boundary; however, if the boundary is too close its effect is to push the electron away from the nucleus. Figure 2(*b*) shows the anisotropic hyperfine splitting as a function of the position of the paraboloidal boundary. It attains its vanishing asymptotic value for $\xi_0 \geqslant 4$, then increases rapidly, reaching a maximum, and drops to zero also rapidly as ξ_0 takes smaller values. The positive sign of A^0_{33} (equation (26*a*)) is an indication of the prolateness of the electron distribution in the confined hydrogen atom. Figure 3 presents the monotonic variation of the electric dipole moment of the hydrogen atom from its asymptotic vanishing value to its infinite value as ξ_0 gets smaller. Such a variation reflects the increasing value of the expectation value for the position of the electron (equation (28)) as the boundary gets closer. Figure 4 illustrates the variations of the pressure of the hydrogen atom on selected points of the paraboloidal boundaries (equation (33), specifically at the vertices, $\rho_2 = 0$, and at the points with $\rho_2 = 1$. The presence of the decreasing exponential functions of ρ_2 in equation (33) ensures that the pressure diminishes rapidly at points on the boundary away from the vertex. The pressure also vanishes asymptotically for distant boundaries, increases, reaches a maximum and then drops to zero as the boundary gets closer.

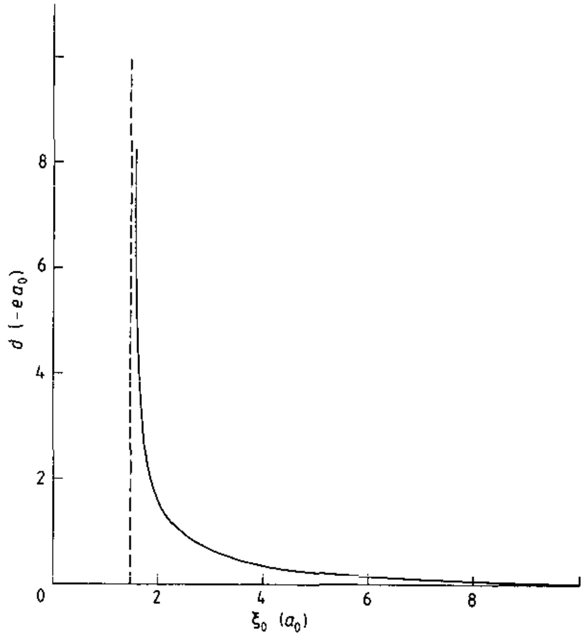

Figure 3. Electric dipole moment of the hydrogen atom in a semi-infinite space bounded by different paraboloidal surfaces.

The study of the hydrogen atom in a semi-infinite space with a paraboloidal boundary is of both intrinsic and practical interest. Its intrinsic value is related to the fact that the quantum system under consideration has an exact solution as shown in this paper. Its utility can be appreciated through a consideration of the atomic properties that have been calculated. The ionization and pressure of the atomic system as functions of the position of the paraboloidal boundary provide physical information relevant

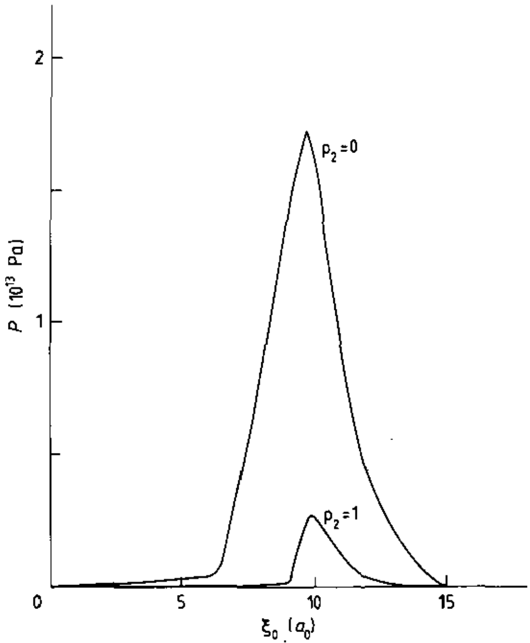

Figure 4. Pressure of the hydrogen atom in a semi-infinite space at vertices ($\rho_2=0$) and at points with $\rho_2=1$ of different paraboloidal surfaces.

for the understanding of the emission of electrons by compressed rocks; the corresponding analysis is to be carried out separately. Comparison of the hyperfine splitting and electric dipole moment of the hydrogen atom in semi-infinite space with the corresponding properties of the free atom or the atom trapped inside a solid gives a way to ascertain and characterize the surface effects. In addition to, but apart from the above, the present work allowed Ley-Koo (1991) to realize that in the hydrogen atom in a strong magnetic field the electron becomes confined inside a paraboloid, thereby breaking parity symmetry.

Appendix

The integrals $T_p(\rho_{10})$ appearing in the anisotropic hyperfine splitting (equation (27b)), can be evaluated by first decomposing the dipole–dipole operator in the integrand into partial fractions:

$$T_p(\rho_{10})=\int_0^{\rho_{10}} \mathrm{d}\rho_1\, \rho_1^p\left(\int_0^\infty \frac{\mathrm{e}^{-2\rho_2}\,\mathrm{d}\rho_2}{(\rho_1+\rho_2)^2}-6\rho_1\int_0^\infty \frac{\mathrm{e}^{-2\rho_2}\,\mathrm{d}\rho_2}{(\rho_1+\rho_2)^3}+6\rho_1^2\int_0^\infty \frac{\mathrm{e}^{-2\rho_2}\,\mathrm{d}\rho_2}{(\rho_1+\rho_2)^4}\right). \tag{A1}$$

Then the integrations over ρ_2 can be carried out by parts and reduced to

$$\int_0^\infty \frac{\mathrm{e}^{-2\rho_2}\,\mathrm{d}\rho_2}{(\rho_1+\rho_2)^2}=\frac{1}{\rho_1}-2E_1(2\rho_1)\,\mathrm{e}^{2\rho_1} \tag{A2}$$

$$\int_0^\infty \frac{\mathrm{e}^{-2\rho_2}\,\mathrm{d}\rho_2}{(\rho_1+\rho_2)^3}=\frac{1}{2\rho_1^2}-\frac{1}{\rho_1}+2E_1(2\rho_1)\,\mathrm{e}^{2\rho_1} \tag{A3}$$

$$\int_0^\infty \frac{\mathrm{e}^{-2\rho_2}\,\mathrm{d}\rho_2}{(\rho_1+\rho_2)^4}=\frac{1}{3\rho_1^3}-\frac{1}{3\rho_1^2}+\frac{2}{3\rho_1}-\tfrac{4}{3}E_1(2\rho_1)\,\mathrm{e}^{2\rho_1} \tag{A4}$$

in terms of the exponential integral function $E_1(x)$ (Abramowitz and Stegun 1965). Substitution of equations (A2)–(A4) in equation (A1) leads to the final form

$$T_p(\rho_{10}) = \int_0^{\rho_{10}} \mathrm{d}\rho_1\, \rho_1^p[4+4\rho_1 - 2(1+6\rho_1+4\rho_1^2)E_1(2\rho_1)\,\mathrm{e}^{2\rho_1}]$$

$$= \frac{4\rho_{10}^{p+1}}{p+1} + \frac{4\rho_{10}^{p+2}}{p+2} - 2\int_0^{\rho_{10}} \mathrm{d}\rho_1\, \rho_1^p(1+6\rho_1+4\rho_1^2)E_1(2\rho_1)\,\mathrm{e}^{2\rho_1} \qquad \text{(A5)}$$

in which the last integral can be evaluated through a Gauss–Legendre quadrature.

References

Abramowitz M and Stegun I A 1965 *Handbook of Mathematical Functions* (New York: Dover)
Atherton N M 1973 *Electron Spin Resonance* (New York: Wiley)
Brady B T and Rowell G A 1986 *Nature* **321** 488
Buckingham R A 1961 *Quantum Theory I. Elements* ed D R Bates (New York: Academic)
Guo Z Q, Zhou D Z, Shih X J, Ma F S, Xi D Y, Cheng C J and Zhou Z W 1988 *Diqiu Wuli Xuebao (Acta Geophysica Sinica)* **31** 566
Hirschfelder J O 1978 *J. Chem. Phys.* **68** 5151
Jiang T F and Shan Y 1985 *J. Phys. C: Solid State Phys.* **18** 3399
Levine J D 1965 *Phys. Rev.* A **140** 586
Ley-Koo E 1991 Submitted for publication
Ley-Koo E and Cruz S A 1981 *J. Chem. Phys.* **74** 4603
Ley-Koo E and Rubinstein S 1979 *J. Chem. Phys.* **71** 351
—— 1980 *J. Chem. Phys.* **73** 887
Ley-Koo E, Shi X J, You J H and Guo Z Q 1989 *Wuli Xuebao (Acta Geophysica Sinica)* **32** 173
Liu Z and Lin D L 1983 *Phys. Rev.* B **28** 4413
Michels A, de Boer J and Nijl A 1937 *Physica* **4** 981
Satpathy S 1983 *Phys. Rev.* B **28** 4585
Shan Y 1987 *J. Phys. B: At Mol. Phys.* **20** 4275
—— 1990 *J. Phys. B: At. Mol. Phys.* **23** L1
Shan Y, Jiang T F and Lee Y C 1985 *Phys. Rev.* B **31** 5487
Shan Y, Lu P C and Tseng H C 1987 *J. Phys. B: At. Mol. Phys.* **20** 4285
Shevtsov G I, Migunov N I, Sobolev G A and Kozlov E V 1975 *Doklady Akademii Nauk SSSP Proc. Academy Sci. USSR) Geophysics* **225** 313
Stephen M J and Auffray J P 1959 *J. Chem. Phys.* **31** 1329